The finite strip method in computational engineering

The Finite Strip Method in Computational Engineering

Dragan D. MILASINOVIC
Assoc. Dean
Faculty of Civil Eng.
Subotica, Yugoslavia

Dragan D. Milasinovic, born 1954, received his Civil Eng. degree from the Univ. of Sarajevo in 1978 and Ph.D. in 1987. He is currently a faculty member at the Univ. of Novi Sad where he is an Assoc. Prof. of Plates and Shells Theory.

Summary

In the last two decades the Finite Strip Method (FSM) has been successfully introduced in the studies of linear behavior, vibrations and buckling as well as nonlinear behavior of various types of prismatic folded plates and curved shells. The reason for the introduction of this method lies in the fact that resolving of several classes of practical problems it is much faster than the more comprehensive and adaptable Method of Finite Elements (FEM). This is generally valid for structures with regular geometrical shape and simple boundary conditions, whose discretization into many finite elements is often very expensive. In such cases the FSM can be extremely competitive in terms of cost and accuracy, both during calculations and in practical application. Discretization of the cross-section into a mesh of finite strips enables the adoption of a finite number of degrees of freedom in the section.

1. The Finite Strip Variational Formulation

The well-known basic procedure of the method is the discretization of plate structures into longitudinal strip elements. The general form of the finite strip displacement function is approximated by the product of polynomes and series which is an interpolation between the classical Ritz and the FEM,

$$f = \sum_{m=1}^{r} Y_m(y) \cdot \sum_{k=1}^{c} N_k(x) \cdot q_{km} \qquad (1)$$

where $Y_m(y)$ are functions from the Ritz and $N_k(x)$ are interpolation functions from the FEM. According to the Green-Lagrange's strain tensor, we present the strain components in an arbitrary point, on the distance z from the middle plane of the plate, as functions of the displacement components of the point of the middle plane of the plate (u_0, v_0, $w=w_0$), as follows:

$$\varepsilon_x = u_{o,x} + \frac{1}{2}\left(u_{o,x}^{\,2} + w_{,x}^{\,2}\right) - z \cdot w_{,xx},$$

$$\varepsilon_y = v_{o,y} + \frac{1}{2}\left(u_{o,y}^{\,2} + w_{,y}^{\,2}\right) - z \cdot w_{,yy}, \qquad (2)$$

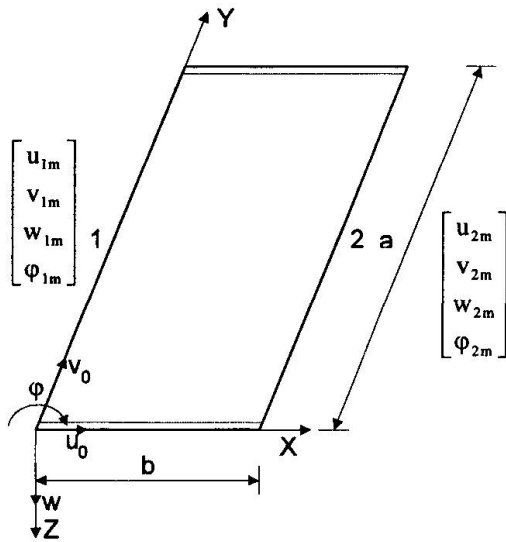$$\gamma_{xy} = u_{o,y} + v_{o,x} + u_{o,y} \cdot u_{o,x} + w_{,x} \cdot w_{,y} - 2 \cdot z \cdot w_{,xy}$$

Fig. 1 A finite strip with eight degrees of freedom

The previous expressions can be obtained as products of the following matrices and vectors:

$$e_o = L_1 A_u \cdot q_u = B_{u1} \cdot q_u$$

$$\eta_o = \frac{1}{2} L_1 \tilde{A}_w \cdot W \cdot L_2 A_w \cdot q_w = \frac{1}{2} B_{w1} \cdot W \cdot B_{w2} \cdot q_w$$

$$\xi_o = \frac{1}{2} L_1 \tilde{A}_u^u \cdot U \cdot L_2 A_u^u \cdot q_u^u = \frac{1}{2} B_{u1}^u \cdot U \cdot B_{u2}^u \cdot q_u^u$$

$$\kappa = L_3 A_w \cdot q_w = B_{w3} \cdot q_w$$

$$e_o^I = L_4 A_u^u \cdot q_u^u = B_{u4}^u \cdot q_u^u$$

$$e_o^{II} = L_5 A_u^v \cdot q_u^v = B_{u5}^v \cdot q_u^v$$

(3)

Where:

$$e_o = \begin{bmatrix} u_{o,x} \\ v_{o,y} \\ u_{o,y} + v_{o,x} \end{bmatrix}, \quad e_o^I = \begin{bmatrix} u_{o,x} \\ 0 \\ u_{o,y} \end{bmatrix}, \quad e_o^{II} = \begin{bmatrix} 0 \\ v_{o,y} \\ v_{o,x} \end{bmatrix},$$

$$\eta_o = \begin{bmatrix} \frac{1}{2} w_{,x}^2 \\ \frac{1}{2} w_{,y}^2 \\ w_{,x} \cdot w_{,y} \end{bmatrix}, \quad \xi_o = \begin{bmatrix} \frac{1}{2} u_{o,x}^2 \\ \frac{1}{2} u_{o,y}^2 \\ u_{o,x} \cdot u_{o,y} \end{bmatrix}, \quad \kappa = \begin{bmatrix} -w_{,xx} \\ -w_{,yy} \\ -2w_{,xy} \end{bmatrix},$$

$$L_1 = \begin{bmatrix} \dfrac{\partial}{\partial x} & 0 \\ 0 & \dfrac{\partial}{\partial y} \\ \dfrac{\partial}{\partial y} & \dfrac{\partial}{\partial x} \end{bmatrix}, \quad L_2 = \begin{bmatrix} \dfrac{\partial}{\partial x} \\ \dfrac{\partial}{\partial y} \end{bmatrix}, \quad L_3 = \begin{bmatrix} -\dfrac{\partial^2}{\partial x^2} \\ -\dfrac{\partial^2}{\partial y^2} \\ -2\dfrac{\partial^2}{\partial x \partial y} \end{bmatrix},$$

(4)

$$L_4 = \begin{bmatrix} \dfrac{\partial}{\partial x} \\ 0 \\ \dfrac{\partial}{\partial y} \end{bmatrix}, \quad L_5 = \begin{bmatrix} 0 \\ \dfrac{\partial}{\partial y} \\ \dfrac{\partial}{\partial x} \end{bmatrix},$$

$$A_u = \begin{bmatrix} A_u^u & 0 \\ 0 & A_u^v \end{bmatrix}, \quad q_u = \begin{bmatrix} q_u^u \\ q_u^v \end{bmatrix}, \quad \tilde{A}_w = \begin{bmatrix} A_w & 0 \\ 0 & A_w \end{bmatrix},$$

$$W = \begin{bmatrix} q_w & 0 \\ 0 & q_w \end{bmatrix}, \quad \tilde{A}_u^u = \begin{bmatrix} A_u^u & 0 \\ 0 & A_u^u \end{bmatrix}, \quad U = \begin{bmatrix} q_u^u & 0 \\ 0 & q_u^u \end{bmatrix}.$$

The total potential energy is defined as the sum of the potential energy of external forces and the strain energy. The formulation of strip characteristics will be presented using the principle of minimum total potential energy.

1.1 Geometrically Nonlinear Viscoelastic Problems

In the non-homogeneous finite strip composed of the layers of concrete and reinforcement, the conditions of balance represent a system of geometrically nonlinear equations.

$$\left[\hat{K}(t) + \tilde{K}(t)\right] \cdot q(t) = D_o(t) \cdot \left[\hat{K}(t_o) + \tilde{K}(t_o)\right] \cdot q(t_o) + Q,$$

(5)

where $\hat{K}$ is the classical or basic stiffness matrix, $\tilde{K}$ the geometrical stiffness matrix.

1.2 Geometrically Nonlinear Elastic Problems

As the instant strains are elastic Eq. (5) can be written in the form:

$$\left[\hat{K}(t_o) + \tilde{K}(t_o)\right] \cdot q(t_o) = Q_o. \tag{6}$$

This is a system of non-linear simultaneous equations at time t=t_0.

1.3 Linear Elastic Problems

By exclusion of the geometrical stiffness matrix from the above equation we obtain a linear system of differential equation.

$$\hat{K}(t_0) \cdot q(t_0) = Q_0. \tag{7}$$

1.4 Linear Viscoelastic Problems

The behavior of the material, which changes with time, can be approximation by the following equations of balance

$$\hat{K}(t) \cdot q(t) = D_0(t) \cdot Q_0 + Q \tag{8}$$

which is a system of linear simultaneous equations, which enclose time dependent effects.

The basic stiffness matrix blocks, together with the geometrical stiffness matrix blocks are used in this interactive analysis:

$$\hat{K}(t) = \begin{bmatrix} \hat{K}_{uu} & \frac{1}{2}\hat{K}_{uw} \\ \frac{1}{2}\hat{K}_{wu} & \hat{K}_{ww} \end{bmatrix},$$

$$\tilde{K}(t) = \begin{bmatrix} 0 & \frac{1}{4}\tilde{K}_{uw} \\ \hline & \frac{1}{2}\tilde{K}_{ww} + \\ \frac{1}{2}\tilde{K}_{wu} & \frac{3}{4}\tilde{K}^{*}_{ww} + \\ & \frac{3}{4}\tilde{K}^{**}_{ww} \end{bmatrix} + \begin{bmatrix} & \frac{1}{4}\tilde{K}^{u}_{uw} + \\ 0 & \frac{1}{2}\tilde{K}^{u*}_{uw} \\ \hline \frac{1}{4}\tilde{K}^{u}_{wu} + & \\ \frac{1}{4}\tilde{K}^{u*}_{wu} & 0 \end{bmatrix} +$$

$$+ \begin{bmatrix} \frac{1}{2}\tilde{K}^{uu}_{uu} + & \\ \frac{3}{4}\tilde{K}^{uu*}_{uu} + & \frac{1}{2}\tilde{K}^{uv}_{uu} \\ \frac{3}{4}\tilde{K}^{uu**}_{uu} & \\ \hline \frac{1}{4}\tilde{K}^{vu}_{uu} & 0 \end{bmatrix} \tag{9}$$

Since the system of equations is nonlinear, the equations of balance in any step of the iterative procedure resolving will not be satisfied. Due to this fact, we shall have the vector of non-balanced forces, i.e., residual loading. It is favorable to present this vector separately for the linear and nonlinear part.

$$R = \hat{R} + \tilde{R} - Q, \tag{10}$$

Q is the load vector and q the vector of nodal line displacement parameters for the finite strip.

$$Q = \begin{bmatrix} Q_u \\ \hline Q_w \end{bmatrix}, q = \begin{bmatrix} q_u \\ q_w \end{bmatrix}, \tag{11}$$

2   Newton-Raphson's   iterative procedure of solution

The variational statement about stationary of the total potential energy in nonlinear problems results in a vector of non-balanced forces,

$$R = \left[\Phi_{,q^{T}}\right] = \left[\hat{K} + \tilde{K}\right] \cdot q - Q = 0, \tag{12}$$

Taylor's expansion of (12) gives:

$$R_1 = R(q_0 + \delta_0) = R(q_0) + \overline{K}_0 \delta_0 + \dots = R_0 + \overline{K}_0 \cdot \delta_0 + \dots \tag{13}$$

where $\overline{K}_0 = R_{,q}$ is the second partial derivative of Φ calculated at q_0 (tangent stiffness matrix).

If (13) is zero and if only the linear terms in q_0 are considered the standard Newton-Raphson iteration is obtained:

$$\delta_0 = -\overline{K}_0^{-1} \cdot R_0. \tag{14}$$

Using this approach, an iteration further gives:

$$\delta_n = -\overline{K}_n^{-1} \cdot R_n, \tag{15}$$

where $\overline{K}_n = R_{,q}$ at q_n.

The criterion for convergence, based on the residual force values, is:

$$\frac{\sqrt{\sum_{i=1}^{N}\left(R_i^n\right)^2}}{\sqrt{\sum_{i=1}^{N}\left(Q_i\right)^2}}\cdot 100 \le \varepsilon \ , \qquad (16)$$

where N is the total number of nodal lines of the decomposed structure, and rt. determines the number of iteration. This criterion means that convergence occurs when the norm of residual forces becomes lesser than ε, which is assigned.

3 Examples

3.1 Example 1

This example presents a comparative analysis of calculations of a prestressed concrete element according to the theory of prestressed concrete within a line analysis, and to the FSM. The results differ considerably, due to two main reasons. First, by the FSM, as opposed to the classical calculation based on the theory of line girders, we can obtain the stress-strain state of the thin-walled bar with open and deformable cross-section. Second, in the calculation of the stress-strain state in an arbitrary time t, the Poynting-Thompson's model of viscoelastic body is used.

Figure 2 presents the cross-section of prestressed concrete element, with the length of 10.20 m.
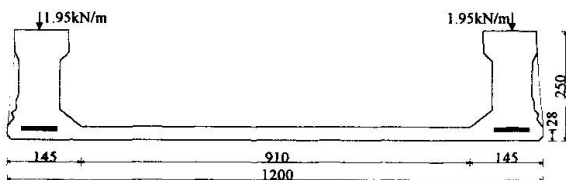

Fig. 2 Cross-section of prestressed concrete element

The element is made of C60, and it is prestressed adhesively with four cables 7ϕ5mm, with total area of 5.5 cm^2 and total initial prestresing force of 667.2 kN. The

allowed stress in steel is 128×10^4 kN/m^2, and the elasticity modulus of steel is $E_t = 2 \times 10^8$ kN/m^2.
Characteristics of concrete as a viscoelastic material are:

$E_c = E_{28} = 4.138 \cdot 10^7$ kN/m^2,

$\varphi(t_\infty, t_o) = 2.8$,

$\chi(t_\infty, t_o) = 0.75$,

$\sigma^p_{allowed} = -18500$ kN/m^2,

$\sigma^t_{allowed} = 2200$ kN/m^2.

Apart from the own weight, the element is subject to live loading which is transmitted to the longitudinal beams. This loading is considered to be movable, and it does not induce the effects of concrete creep. The loading on two beams is 3.9 kN/m. In combination with the own weight, if it is also considered as line loading, the loading on both beams is 6.0 kN/m. Figure 3. presents the mesh of finite strips with the corresponding boundary conditions.
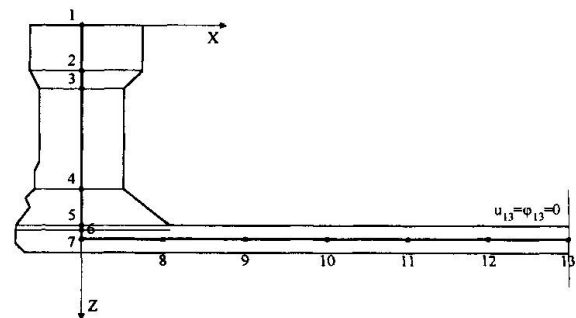

Fig. 3 Mesh of finite strips and symmetry conditions

The results of calculation are presented in Figure 4 (a), (b) and (c). In Figure 4(a) the diagram drawn in the full line represents σ_y caused by own weight and prestressing in the time t_0, while the dotted line is for the time t_∞. The stresses are calculated in the middle of the span length. Figure 4(b) presents the diagram of σ_y caused by the live loading, and Figure 4(c) of that caused by the total loading and prestressing in the time t_∞.

It can be seen that the stresses in the concrete exceed the allowed values. The line analysis, which can not yield good results for such a cross-section, gives stress values which are within the allowed limits. According to this calculation, in the upper
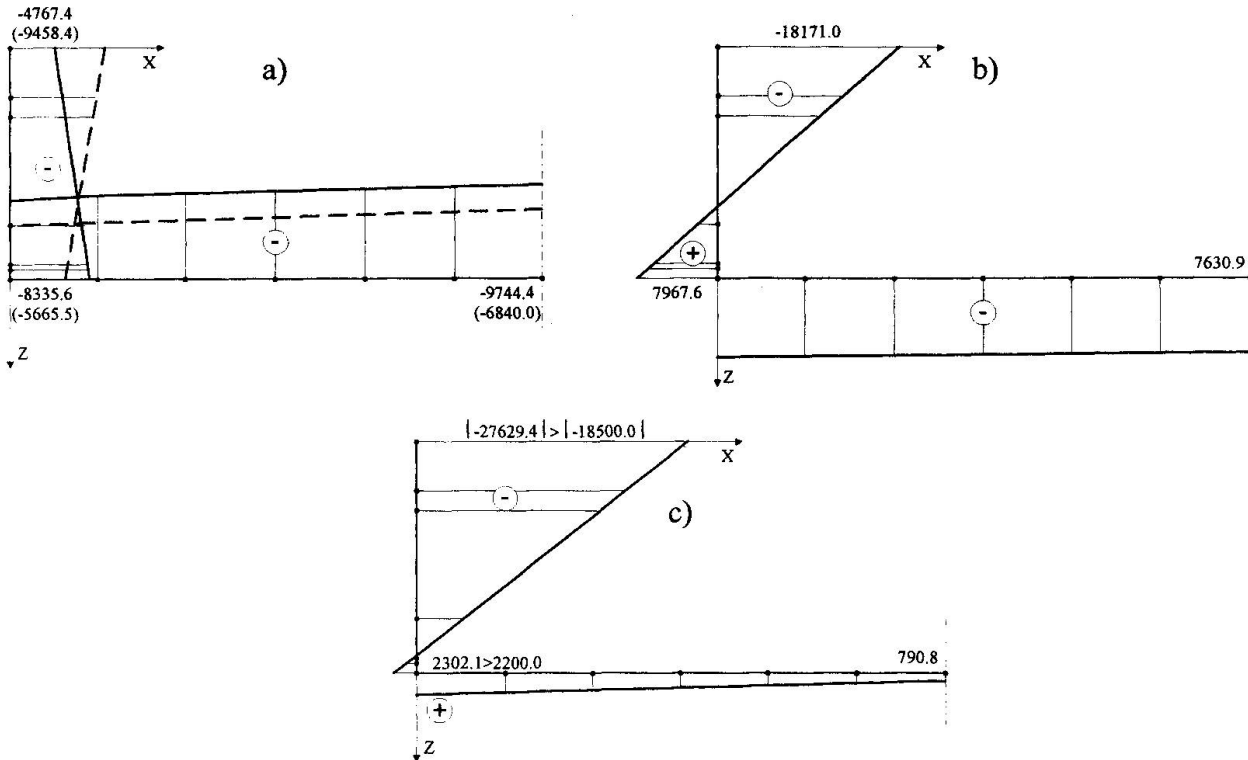
Fig. 4 Diagrams of stress σ_y in the middle of girder span length, (a) effect of own weight and prestressing in t_0 and t_∞ (b) effect of live loading, (c) effect of own weight, prestressing and live loading in t_∞

fibre $\sigma_y{}^p = -18310$ kN/m^2, and in the lower fibre $\sigma_y{}^t = 616$ kN/m^2.

In addition, it should be noted that according to the FSM, the loss of prestressing force caused by elastic strains of concrete (3.23%) and elastic strains and creep of concrete (6.99%) is much lesser than the total prestressing force loss anticipated in the calculation according to the line analysis (20%).

3.2 Example 2

Prefabricated prestressed concrete girders are complex elements, 75 x 210 cm, lightened by three openings $\phi 50$ cm. The elements are from 13.40 to 25.40 m long, see Figure 5 and they serve as bridge girders. They are made of the following materials:

- steel for prestressing 1800/1600, with nominal cross-section of 0.93 cm^2,
- concrete C40.

The cutting of tendons can be carried out only when the concrete reaches the strength of 30 MN/m^2. The reason for this is the

unfavorable stress state of the girder in the moment of prestressing. Here we shall
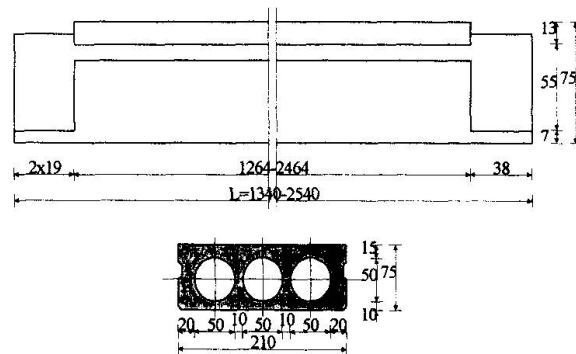

Fig. 5 View and cross-section of bridge girder

analyze a girder, which is 19.50m long, prestressed with 48 tendons with total area of 44.64 cm^2, and total initial prestressing force of 5625 kN.

The mesh of finite strips in the cross-section

of the girder is presented in Figure 6.
Polyhedral shell finite strips with eight
degrees of freedom were used. Eleven terms
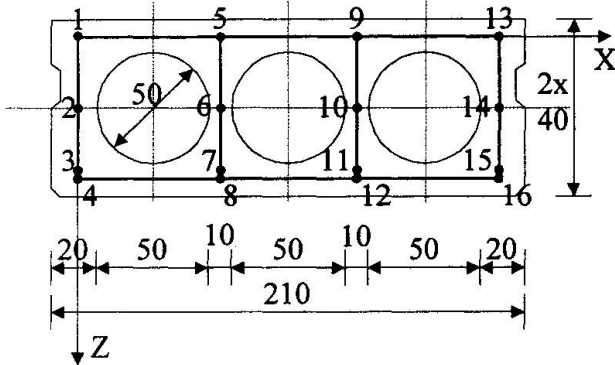of the series were used in the calculation of
own weight and prestressing.

Fig. 6 Mesh of finite strips in the cross-section of girder

Figure 7 presents the most unfavorable
distribution of the stress σ_y in the node lines
1 and 3. Tension stress is unfavorable for
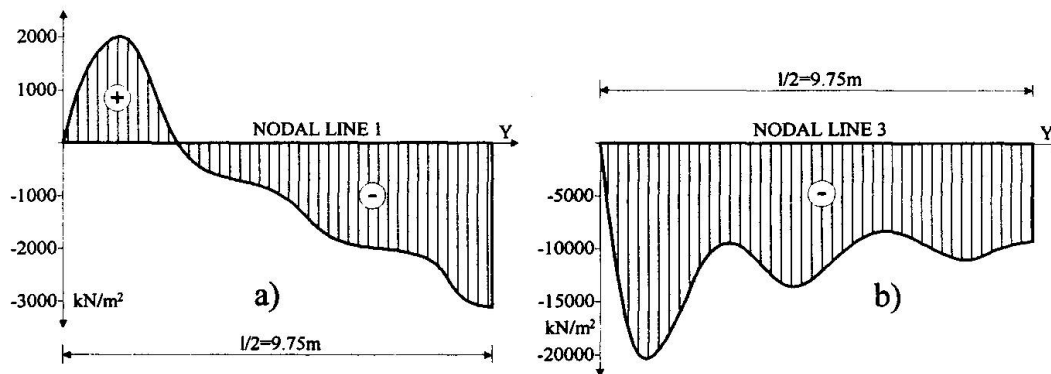node line 1, and high stress of pressure for
node line 3

displacement amplitudes. Complex
mathematical expressions were programmed
within the frame of the standard Newton-
Raphson's iterative procedure. The
application of the FSM promises more
reliable results than the application of the
FEM, since the errors of discretization in the
former method are much lesser. Bearing in
mind that the FSM is a semi-analytical and
semi-numerical method, in the theory of
polyhedral shells, we find it very favorable
in solving of this problem.

References

1. Cheung, Y.K., "The Finite Strip Method
   in Structural Analysis", Oxford,
   Pergamon Press, 1976.
2. Loo, W.C., Causeus, A.R., "The Finite
   Strip Method in Bridge Engineering",
   Wexham Springs, Viewpoint
   Publications (C&CA), 1978.
3. Milašinović, D.D., "The Finite Strip
   Method in Computational Mechanics,
   Faculty of Civil Engineering: Subotica,
   Budapest, Belgrade, 1997

Fig. 7 Distribution of stress σ_y (kN/m²); (a) in node line 1, (b) in node line 3

5   Conclusions

A nonlinear FSM has been presented for use
in the design of reinforced concrete plate
structures. The procedure has advantages
over the conventional FEM, since the
application of numerical integration is
avoided, and the stiffness matrices, loading
vectors and residual forces are expressed
explicitly as a function of the nodal